Inorg. Chem. **2007**, *46*, 3144–3153

Copper Complexes of New Benzodioxotetraaza Macrocycles with Potential Applications in Nuclear Medicine

Patricia Antunes,[†,‡] Rita Delgado,*[,†,§] Michael G. B. Drew,[∥] Vitor Félix,[⊥] and Helmut Maecke[‡]

Instituto de Tecnologia Química e Biológica, UNL, Apartado 127, 2781-901 Oeiras, Portugal, Division of Radiological Chemistry, Department of Radiology, University Hospital Basel, Switzerland, Instituto Superior Técnico, Av. Rovisco Pais, 1049-001 Lisboa, Portugal, Department of Chemistry, University of Reading, Whiteknights, Reading, UK RG6 6AD, and Departamento de Química, CICECO, Universidade de Aveiro, 3810-193 Aveiro, Portugal

Received November 15, 2006

Two novel benzodioxotetraaza macrocycles [2,9-dioxo-1,4,7,10-tetraazabicyclo[10.4.0]1,11-hexadeca-1(11),13,15-triene (H_2**L1**) and 2,10-dioxo-1,4,8,11-tetraazabicyclo[11.4.0]1,12-heptadeca-1(12),14,16-triene (H_2**L2**)] were synthesized by a [1 + 1] crablike cyclization. The protonation constants of both ligands were determined by ^{1}H NMR titration and by potentiometry at 25.0 °C in 0.10 M ionic strength in KNO_3. The latter method was also used to ascertain the stability constants of their copper(II) complexes. These studies showed that the Cu**L1** complex has a much lower thermodynamic stability than the Cu**L2**, and the H_2**L2** displays an excellent affinity for copper(II), due to the good fit of copper(II) into its cavity. The copper complexes of the novel ligands were characterized by electronic spectroscopy in solution and by crystal X-ray diffraction. These studies indicated that the copper center in the Cu**L1** complex adopts a square–pyramidal geometry with the four nitrogen atoms of the macrocycle forming the equatorial plane and a water molecule at axial position, and the copper in the Cu**L2** complex is square–planar. Several labeling conditions were tested, and only H_2**L2** could be labeled with ^{67}Cu efficiently (>98%) in mild conditions (39 °C, 15 min) to provide a slightly hydrophilic radioligand (log $D = -0.19 \pm 0.03$ at pH 7.4). The in vitro stability was studied in the presence of different buffers or with an excess of diethylenetriamine-pentaethanoic acid. Very high stability was shown under these conditions for over 5 days. The incubation of the radiocopper complex in human serum showed 6% protein binding.

Introduction

The unique properties of ligands that are a result of the replacement of an amine by an amide in polyazamacrocycles derive from their dual features between oligopeptides and saturated cyclic amines. These compounds are able to coordinate divalent metal cations, such as Ni^{2+} or Cu^{2+}, by displacing the amide protons.[1,2] The resulting complexes are of considerable interest as functional catalysts, biological models for metalloproteins, and in oxygen uptake.[3,4] Furthermore, the research of neutral copper complexes of this type of ligand for nuclear medicine applications is a stimulating, continuous endeavor.[2,5] The alliance of their structural features with the versatile and unique radiophysical properties of copper radioisotopes[6−11] leads to their potential usefulness in diagnostic and/or therapeutic applications.[5]

* E-mail: delgado@itqb.unl.pt.
† Instituto de Tecnologia Química e Biológica.
‡ University Hospital Basel.
§ Instituto Superior Técnico.
∥ University of Reading.
⊥ Universidade de Aveiro.

(1) Fabbrizzi, L.; Kaden, T. A.; Perotti, A.; Seghi, B.; Siegfried, L. *Inorg. Chem.* **1986**, *25*, 321.
(2) Motekaitis, R. J.; Sun, Y.; Martell, A. E.; Welch, M. *Can. J. Chem.* **1999**, *77*, 614.
(3) Machida, R.; Kimura, E.; Kodama, M. *Inorg. Chem.* **1983**, *22*, 2055.
(4) Meyer, M.; Frémond, L.; Espinosa, E.; Guilard, R.; Ou, Z.; Kadish, K. M. *Inorg. Chem.* **2004**, *43*, 5572.
(5) Cutler, C. S.; Wuest, M.; Anderson, C. J.; Reichert, D. E.; Sun, Y.; Martell, A. E.; Welch, M. J. *Nucl. Med. Biol.* **2000**, *27*, 375.
(6) Smith, S. A. *J. Inorg. Biochem.* **2004**, *98*, 1874.
(7) Lewis, J. S.; Lewis, M. R.; Srinivasan, A.; Schmidt, M. A.; Wang, J.; Anderson, C. J. *J. Med. Chem.* **1999**, *42*, 1341.
(8) McQuade, P.; Miao, Y.; Yoo, J.; Quinn, T. P.; Welch, M. J.; Lewis, J. S. *J. Med. Chem.* **2005**, *48*, 2985.
(9) Morphy, J. R.; Parker, D.; Kataky, R.; Eatom, M. A. W.; Millican, A. T.; Alexander, R.; Harrison, A.; Walker, C. *J. Chem. Soc. Perkin Trans. 2* **1990**, 573.
(10) Heppeler, A.; Froidevaux, S.; Eberle, A. N.; Maecke, H. R. *Curr. Med. Chem.* **2000**, *7*, 971.
(11) Novak-Hofer, I.; Zimmermann, K.; Maecke, H.; Amstutz, H. P.; Carrel, F.; Schubiger, P. *J. Nucl. Med.* **1997**, *38*, 536.

10.1021/ic062172o CCC: $37.00 © 2007 American Chemical Society
Published on Web 03/23/2007

Scheme 1

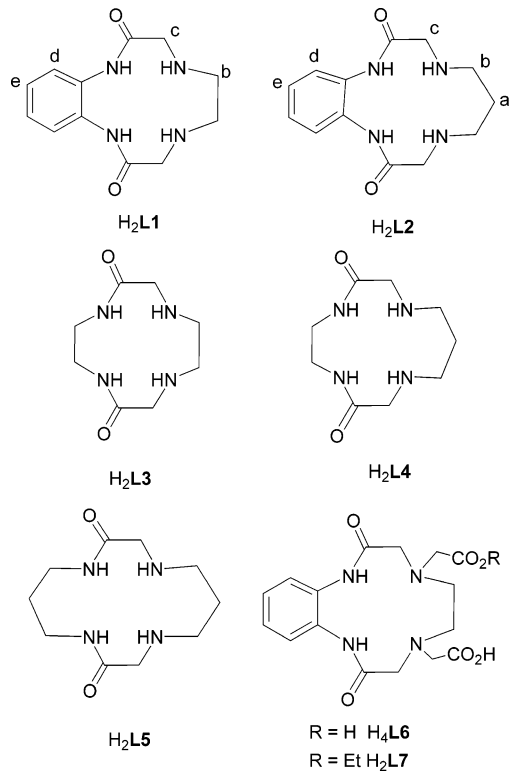

Among several copper radionuclides, the longest-lived ^{67}Cu is of interest for its medium energy β-emissions and its γ-rays that permit imaging of radioactivity distribution during therapy. To further investigate the chemistry of dioxotetraaza macrocycles and their potential usefulness as radiolabeled copper complexes in nuclear medicine, a benzene ring was introduced into the backbone of that class of ligands (Scheme 1). The consequent rigidity of the molecular skeleton confers spatial preorganization to the donor atoms, which usually leads to a more efficient complexation and slower complex dissociation.[12−17] Moreover, functionalization of the benzene ring can be easily achieved,[18] which allows it to be coupled with any type of biomolecule (e.g., peptide or antibody), and it also lessens the influence of the coordination sphere on the biological vector.

In the present study, the syntheses of the 12- and 13-membered macrocyclic benzodioxotetraamine chelators 2,9-dioxo-1,4,7,10-tetraazabicyclo[10.4.0]1,11-hexadeca-1(11),13,15-triene (H_2**L1**) and 2,10-dioxo-1,4,8,11-tetraaza-bicyclo[11.4.0]1,12-heptadeca-1(12),14,16-triene (**(**H_2**L2**) (Scheme 1) are described. The binding ability of both ligands to copper(II) was evaluated by potentiometric measurements, and the complexes were characterized by electronic spectroscopy in solution and by crystal X-ray diffraction determinations. The complexation with ^{67}Cu was evaluated, and several stability tests such as serum stability were performed.

Experimental Section

Caution! *Although no problems were found in this work, metal perchlorate salts mixed with organic ligands and solvents are potentially explosive and should be prepared and handled only in small quantities and with great care.*

Instrumentation. Microanalyses were carried out by the ITQB Microanalytical Service. IR spectra were recorded from KBr pellets on a UNICAM Mattson 7000 spectrometer. Electronic spectra were recorded on a Cary 500 version 8.01 spectrophotometer. Electron paramagnetic resonance (EPR) spectra were recorded with a Bruker EMX300 spectrometer that was equipped with continuous-flow cryostats for liquid nitrogen and operated at the X-band. ^{1}H and ^{13}C NMR spectra were recorded with a Bruker AMX-300 spectrometer at probe temperature. Melting points were determined on a BÜCHI 530 apparatus and were uncorrected. Electrospray ionization mass spectrometry (ESI-MS) was obtained from a Finnigan SSQ 7000 spectrometer. Analytical reversed-phase high-performance liquid chromatography (RP-HPLC) was carried out on a Hewlett-Packard 1050 HPLC system (Waldbronn, Germany) that was coupled to a multiwavelength detector and a flow-through Berthold LB506C1 γ-detector. Analytical RP-HPLC was performed using Uptisphere 5 C18 columns, 250 × 4.6 mm, from Interchrom, with an eluent system of various mixtures of 10% ammonium acetate in H_2O (solvent A) and MeOH (solvent B). Quantitative γ−counting was performed on a COBRA 5003 γ-system well counter from Packard Instrument (Switzerland).

Reagents. *O*-Phenylenediamine, bromoacetyl chloride, ethylenediamine, and propylenediamine were obtained from Aldrich Chemical Co. Solvents were either used as purchased or were dried according to standard procedures.[19] The reference signal used for the ^{1}H NMR measurements in D_2O was 3-(trimethylsilyl)-propanoic acid d_4-sodium salt, and in $CDCl_3$ and deuterated dimethyl sulfoxide (DMSO-d_6) the solvent itself was used as reference. For ^{13}C NMR spectra in D_2O, dioxane was used as the internal reference. A solution of $^{67}CuCl_2$ was obtained from the Paul Scherrer Institute.

Synthesis of 2-Chloro-*N*-[2-(2-chloro-acetylamino)-phenyl]-acetamide. A solution of *o*-phenylenediamine (1.08 g, 0.01 mol) in anhydrous dimethylformamide (DMF, 7.5 mL) and anhydrous dioxane (7.5 mL) was cooled to 0 °C, under nitrogen. Bromoacetyl chloride (3.19 g, 0.02 mol) was added dropwise to the mixture while keeping the internal temperature below −5 °C. After addition of the bromoacetyl chloride (∼35 min), the reaction mixture was stirred overnight at room temperature (RT). Water (28 mL) was added to the mixture, from which precipitated a light pink compound that was filtered, washed once with 5% HBr, washed several times with water (56 mL), and then dried to produce the title compound (3.36 g, 96%). ^{1}H NMR (DMSO-d_6, ppm): 9.71 (br s, 2 H), 7.54−7.51 (m, 2 H), 7.23−7.19 (m, 2 H), and 4.12 (s, 4 H). ^{13}C NMR (DMSO-d_6, ppm): 165.09, 130.19, 125.49, 124.87, and 30.10.

Synthesis of H_2L1. A mixture of 2-chloro-*N*-[2-(2-chloro-acetylamino)-phenyl]-acetamide (1.75 g, 0.005 mol), ethylenedi-

(12) Antunes, P.; Campello M. P.; Delgado, R.; Drew, M. G. B.; Félix, V.; Santos, I. *J. Chem. Soc. Dalton Trans.* **2003**, 1852.
(13) Lacerda, S.; Campello, M. P.; Santos, I. C.; Santos, I.; Delgado, R. *Polyhedron* **2005**, *24*, 451.
(14) Fossheim, R.; Dugstad, J. H.; Dahlf, S. G. *J. Med. Chem.* **1991**, *34*, 819.
(15) Rauganathan, R. S.; Pillai, R. K.; Raju, N.; Fan, H.; Nguyen, H.; Tweedle, M. F.; Desreux, J. F.; Jacques, V. *Inorg. Chem.* **2002**, *41*, 6846.
(16) McMurry, T. J.; Pippin, C. G.; Wu, C.; Deal, K. A.; Brechbiel, M. W.; Mirzadeh, S.; Gansow, O. A. *J. Med. Chem.* **1998**, *41*, 3546.
(17) Chong, H. S.; Garmestani, K.; Bryant, L. H.; Brechbiel, M. W. *J. Org. Chem.* **2001**, *66*, 7745.
(18) Reany, O.; Gunnlaugsson, T.; Parker, D. *J. Chem. Soc. Perkin Trans. 2* **2000**, 1819.
(19) Amarego, D. D.; Perrin, W. L. F. *Purification of Laboratory Chemicals*, Pergamon: Oxford, 1988.

amine (0.274 mL, 0.005 mol), and potassium carbonate (8.48 g, 0.080 mol) in acetonitrile (250 mL) was stirred at 40 °C for 24 h and additionally for 24 h at RT. The mixture was filtered, and the filtered solvent was evaporated until 40 mL remained. The yellow solution was left overnight at 0 °C; the crystals that were obtained were collected and washed several times with acetonitrile (0.32 g, 26%). Only once was it possible to obtain crystals. All other attempts to repeat the procedure reported herein yielded a white powder as the resulting compound. The reason for this observation remains unknown. Mp: 190−192 °C. Anal. Calcd for $C_{12}H_{16}N_4O_2$: C, 58.05; H, 6.50; N, 22.57. Found: C, 58.52; H, 6.84; N, 22.68. MS (ESI) (*m/z*): 249.1 ($[M + H]^+$). ^{1}H NMR (D_2O, ppm): 7.51−7.41 (m, 4 H), 3.41 (s, 4 H), and 2.79 (s, 4H). ^{13}C NMR (D_2O, ppm): 174.14, 129.69, 127.27, 125.52, 51.63, and 47.61.

Synthesis of H_2L2. A mixture of 2-chloro-N-[2-(2-chloro-acetylamino)-phenyl]-acetamide (1.75 g, 0.005 mol), propylenediamine (0.274 mL, 0.005 mol), and potassium carbonate (8.48 g, 0.080 mol) in acetonitrile (250 mL) was stirred at 40 °C for 24 h. After the mixture was cooled, it was filtered and the solvent was evaporated to dryness. The yellow compound was washed several times with acetonitrile, until a white powder was obtained (0.68 g, 52%). Mp: 219−220 °C. Anal. Calcd for $C_{13}H_{18}N_4O_2 \cdot 0.5\ H_2O$: C, 59.53; H, 6.92; N, 21.36. Found: C, 59.44; H, 7.02; N, 21.39. MS (ESI) (*m/z*): 263.1 ($[M + H]^+$). ^{1}H NMR (D_2O, ppm): 7.63−7.59 (m, 4 H), 7.37−7.36 (m, 2 H), 3.42 (s, 4 H), 2.84−2.80 (t, 4 H), and 1.71−1.65 (q, 2 H). ^{13}C NMR (D_2O, ppm): 165.83, 131.78, 129.68, 128.42, 46.95, 44.55, and 19.85.

Synthesis of [CuL1(H_2O)]. The compound H_2**L1** (1.2 mg, 2.41 × 10^{-3} M) was dissolved in 2 mL of a 1.0 M aqueous solution of $NaClO_4$, and a portion of $Cu(NO_3)_2$ (0.1 mL, 0.0399 M) was added. The pH was adjusted to 10. The flask was sealed, and after 2−3 days some blue, single crystals were obtained.

Synthesis of [CuL2)]. A solution of $Cu(NO_3)_2$ (0.095 mL, 0.0399 M) was added to a solution of H_2**L2** (1.0 mg, 1.9 × 10^{-3} M) in 2 mL of 1.0 M $NaClO_4$ at pH 8. The flask was sealed, and after 2 days some purple, single crystals were obtained.

Potentiometric Measurements. Reagents and Solutions. Solutions containing approximately 0.025 M of metal ion were prepared from the nitrate salts of the metals and were titrated using standard methods.[20] Demineralized water (Millipore/Milli-Q System) was used. Carbonate-free solutions of the titrant, KOH, were obtained, maintained, and discarded as described.[12−13]

Equipment and Work Conditions. The equipment was used as described previously.[21] The temperature was kept at 25.0 ± 0.1 °C, and atmospheric CO_2 was excluded from the cell during the titrations by passing purified nitrogen across the top of the experimental solution in the reaction cell. The ionic strength of the solutions was kept at 0.10 ± 0.01 M in KNO_3.

Measurements. The $[H^+]$ of the solutions was determined by the measurement of the electromotive force (emf) of the cell, $E = E'^\circ + Q \log[H^+] + E_j$. E'°, Q, E_j, and $K_w = ([H^+][OH^-])$ were obtained as described previously.[12,13,21] The term pH is defined as $-\log [H^+]$. The value of K_w was determined to be equal to $10^{-13.80}$ M^2.[12,13,21] The potentiometric equilibrium measurements were made using 20.00 mL of 2.5 × 10^{-3} to 3.8 × 10^{-3} M chelator solutions that were diluted to a final volume of 25.00 mL in the absence of metal ions and in the presence of copper metal ions for which the C_M/C_L ratio was 1:1 and 1:2. A minimum of two replicate measurements were taken. The emf data were taken after addition of 0.050 mL increments of standard KOH 0.1 M solution, and after stabilization in this direction, equilibrium was then approached from the other direction by the addition of a standard 0.1 M HNO_3 solution.

Table 1. Crystal Data and Pertinent Refinement Details for Compounds H_2**L1**, [Cu**L1**(H_2O)], and [Cu**L2**]

	H_2**L1**	[Cu**L1**(H_2O)]	[Cu**L2**]
empirical formula	$C_{12}H_{16}N_4O_2$	$C_{12}H_{18}CuN_4O_4$	$C_{13}H_{18}CuN_4O_3$
mol wt	248.29	345.84	341.85
crystal system	monoclinic	monoclinic	monoclinic
space group	$P2_1/a$	$P2_1$	$P2_1/n$
a / [Å]	9.1455(13)	6.7710(18)	9.0390(10)
b / [Å]	8.4625(12)	10.2050(15)	15.0319(17)
c/[Å]	15.810(2)	10.2277(14)	9.9870(9)
β/[°]	103.570(13)	103.509(17)	95.586(8)
V [Å^3]	1189.4(3)	687.2(2)	1350.5(2)
Z	4	2	4
D_c [Mg·m^{-3}]	1.387	1.671	1.681
μ/[mm^{-1}]	0.098	1.612	1.634
reflections collected	7489	5572	9479
unique reflections, [R_{int}]	3422 [0.0242]	4285 [0.0520]	3937 [0.0409]
refined parameters	176	203	198
final *R* indices			
R_1, wR_2 [$I > 2\sigma I$]	0.1060, 0.3150	0.0570, 0.1140	0.0340, 0.0699
R_1, wR_2 (all data)	0.1367, 0.3254	0.0864, 0.1207	0.0647, 0.0727

Calculations of Equilibrium Constants. Overall protonation ($\beta_{H_hL_l}$) and stability constants ($\beta_{M_mH_hL_l}$) were calculated with the HYPERQUAD program,[22] with $\beta_{M_mH_hL_l} = [M_mH_hL_l]/[M]^m[H]^h[L]^l$. The quoted errors are the standard deviations of the overall stability constants given directly by the program for the input data that include all the experimental points of all titration curves.

^{1}H NMR Spectroscopic Measurements. The assessment of the protonation constants was also performed by ^{1}H NMR titrations, using 0.01 M ligand solutions in D_2O. The pD was adjusted by the addition of DCl or of CO_2-free KOD with an Orion 420A instrument fitted with a combined Hamilton SpinTrode microelectrode. The pH* was measured directly in the NMR tube, after the microelectrode was calibrated with buffered aqueous solutions. The final pD was calculated from pD = pH* + (0.40 ± 0.02), where pH* is the reading in the pH meter.[23] The protonation constants in D_2O were calculated by using the program HYPNMR.[24]

Spectroscopic Studies. For electronic spectra, aqueous solutions of the complexes were prepared by the addition of copper(II) nitrate to the ligand. Adjustment to the appropriate pH value with aqueous solutions of KOH and HNO_3 was performed. EPR spectroscopy measurements of the copper(II) complexes were recorded at 96 K. The complexes were prepared by the 1:1 v/v mixture of DMSO and a 2.0 × 10^{-3} M aqueous solution of the copper complex in 1.0 M $NaClO_4$ at pH 6.5, 8, and 10.

X-ray Diffraction Determinations. The pertinent crystallographic X-ray data for compounds **1**, **2**, and **3** are listed in Table 1. X-ray data were collected at 150 K on a CCD X-Calibur machine using graphite monocromatized Mo−Kα radiation (λ = 0.71073 Å) at Reading University. The crystals were positioned 50 mm from the CCD. A total of 321 frames were measured with a counting time of 3 s. Data analyses were carried out with the Crysalis program.[25] Empirical absorption corrections were carried out using the Abspack program.[26]

(20) Schwarzenbach, G.; Flaschka, W. *Complexometric Titrations*, Methuen & Co: London, 1969.
(21) Marques, F.; Gano, L.; Campello, M. P.; Lacerda, S.; Santos, I.; Lima, L. M. P.; Costa, J.; Antunes, P.; Delgado, R. *J. Inorg. Biochem.* **2006**, *100*, 270.
(22) Gans, P.; Sabatini, A.; Vacca, A. *Talanta* **1996**, *43*, 1739.
(23) Covington, A. K.; Paabo, M.; Robison, R. A.; Bates, R. G. *Anal. Chem.* **1968**, *40*, 700.
(24) Frassineti, C.; Ghelli, S.; Gans, P.; Sabatini, A.; Moruzzi, M. S.; Vacca, A. *Anal. Biochem.* **1995**, *231*, 374.

The structures were solved by direct methods and subsequent difference Fourier syntheses and were refined by a full matrix least-squares on F^2 using the SHELX−97 system programs.[27] Anisotropic thermal parameters were used for all non-hydrogen atoms. The hydrogen atoms bonded to carbon atoms in all compounds and the hydrogen atoms bonded to nitrogen atoms in **2** and **3** were included in the refinement of calculated positions. The hydrogen atoms bonded to nitrogen atoms in **1** and the atomic positions of hydrogen atoms of water molecules in **2** and **3** were revealed from the final difference Fourier maps. All hydrogen atoms were refined with isotropic temperature factors equivalent to 1.2 times those of the atom to which they were attached. Furthermore, the O−H distances were restrained to 0.82 Å. The residual electronic density found for all compounds, listed in Table 1, are within the expected range. Molecular diagrams were drawn with PLATON.[28]

Preparation of ^{67}Cu−Ligand Complexes. A solution of $^{67}CuCl_2$ was added either to a 5.0×10^{-3} M or to a 1.0×10^{-3} M ligand solution in 100 μL of 0.1 M ammonium acetate (pH from 5.5 to 8.0) buffer solution. The radiolabeling efficiency was tested by using an array of temperatures and reaction times. Radiochemical purity was determined by analytical RP−HPLC (flow: 0.75 mL/min) for all of the ^{67}Cu−ligand complexes prepared. The eluent and gradient system used was as follows: solvent A: 10% ammonium acetate in H_2O, solvent B: MeOH; 0−5 min, 50% B; 5−10 min, 50−100% B; 10−15 min, 100% B; 15−20 min 100−50% B. A quality control was performed by taking an aliquot of the labeled samples (5 μL) and adding a large excess of diethylenetriamine-pentaethanoic acid (DTPA). The unlabeled copper could be identified by analytical HPLC as the ^{67}Cu-labeled DTPA complex. If one peak was visualized, a second quality control was performed by co-injecting that aliquot with a ^{67}Cu-labeled DTPA solution.

Stability of ^{67}Cu−Complexes in Aqueous Solutions. The radiolabeled complex (10 μL) was added to 100 μL of different aqueous solutions, namely, saline, phosphate buffered saline (PBS, pH 7.4), 0.1 M ammonium acetate at various pH values (5.5, 6.4, and 8.0), and tris buffer (pH 7.4). Also, a competition experiment with a 100-fold excess of DTPA or with a 50-fold excess of $CuCl_2$ was performed. The mixtures were incubated at 37 °C for up to 5 days. At various time points, an aliquot of sample was taken and evaluated by analytical RP−HPLC, with the eluent and gradient described above.

Serum Stability and Protein Binding. To 1.0 mL of freshly prepared human serum, previously equilibrated in a 5% CO_2 (95% air) environment at 37 °C, 10 μL of 5×10^{-3} M ^{67}Cu-labeled ligands were added. The mixture was incubated in a 5% CO_2, 37 °C environment. At different time points, 100 μL aliquots (in triplicate) were removed and treated with 200 μL of EtOH. Samples were then cooled (4 °C) and centrifuged for 15 min at 500*g* and 4 °C to precipitate serum proteins. The supernatants were removed and the sediment was washed twice with 1 mL of EtOH. The activity in the ethanolic phase and in the proteic precipitate was measured in a γ-counter. An excess of DTPA was added to the proteic fraction collected at the 2 h time point to verify, by analytical HPLC, if transchelation had occured. Both counts were compared to give the percentage of ^{67}Cu complexes not bound to proteins or the percentage of radiometal transferred to serum proteins. The supernatant was checked by analytical HPLC.

(25) Crysalis, Oxford Diffraction Ltd, Version 1, 2005.
(26) Abspack, Oxford Diffraction Ltd, 2005.
(27) Sheldrick, G. M. *SHELX−97*, University of Göttingen, Göttingen, Germany, 1997.
(28) Spek A. L. *PLATON, a Multipurpose Crystallographic Tool*; Utrecht University, Utrecht, The Netherlands, 1999.

Table 2. Protonation Constants of $\mathbf{L1}^{2-}$−$\mathbf{L5}^{2-}$ [a]

equilibrium	$\mathbf{L1}^{2-}$ [b]	$\mathbf{L2}^{2-}$ [b]	$\mathbf{L3}^{2-}$ [c]	$\mathbf{L4}^{2-}$ [c]	$\mathbf{L5}^{2-}$ [c]
$HL^- + H^+ \rightleftarrows H_2L$	11.56(5)	11.51(1)			
$HL^- + 2H^+ \rightleftarrows H_3L^+$	17.69(6)	18.33(2)	6.98	7.69	7.81
$HL^- + 3H^+ \rightleftarrows H_4L^{2+}$	20.54(4)	23.83(1)	10.73	13.59	13.49
$H_2L + H^+ \rightleftarrows H_3L^+$	6.13	6.82	6.98	7.69	7.81
$H_3L^+ + H^+ \rightleftarrows H_4L^{2+}$	2.85	5.50	3.75	5.90	5.68

[a] $T = 25$ °C; $I = 0.10$ M in KNO_3. [b] Values in parentheses are standard deviations in the last significant figures. [c] $I = 0.10$ M in KCl, ref 2.

Determination of Partition Coefficient (pH 7.4). The partition coefficient (log *D*) of [^{67}Cu**L2**] was determined by adding 10 μL of the labeled complex to a solution containing 500 mL of octanol and 500 mL of PBS (obtained from saturated octanol/PBS solutions). The resulting solutions were then shaken for 1 h at RT. After equilibration for a few minutes, the mixtures were centrifuged (10 min at 2000 rpm) to achieve good separation. The activity concentrations in 100 μL samples of both the aqueous and the organic phase were measured in a γ−counter. The lipophilicity was calculated as the average log ratio value of the radioactivity in the organic fraction and the PBS fraction from the 6 samples.

Results and Discussion

Syntheses. Macrocycles H_2**L1** and H_2**L2** (Scheme 1) were synthesized by a crablike cyclization, involving condensation of a bis-(chloroacetamide) and the corresponding ethylenediamine or propylenediamine. This [1 + 1] cyclization seems to be favored for the less conformational strained backbone of H_2**L2** as compared to H_2**L1**. Nevertheless, these ligands were prepared in good overall yields: 61% for H_2**L1** and 74% for H_2**L2**.

Acid−Base Behavior. The acid−base behavior of the two ligands was investigated through potentiometry and ^{1}H NMR spectroscopy. Three out of four protonation constants for both macrocycles that were fully deprotonated could be determined; one amide proton is too basic to be determined in water or even in D_2O by ^{1}H NMR spectroscopy. Indeed, due to the withdrawing effect of the benzene ring directly connected to the amides, these groups become more acidic, and therefore it was expected that the determination of all the protonation constants of these macrocycles was possible. However, the expectations were not confirmed. The corresponding values are reported in Table 2 along with the ones of related dioxotetraaza macrocycles.[2]

For H**L1**$^-$ and H**L2**$^-$, the first protonation occurs in one of the amides and the next two are ascribed to the two amine centers. As expected, the second and the third protonation constants found for the new benzodioxotetraaza macrocycles are of the same order of magnitude of the values previously reported for the related compounds, H_2**L3** and H_2**L4**. The second and third constants are lower than expected for amine centers, but the proximity of the amide groups causes the amines to be much more acidic. Additionally, the relative magnitude of the last protonation constant reflects factors such as the electrostatic repulsion between two positive charges, hydrogen bond formation or breaking, or a conformational rearrangement of the ligand framework. In this sense, among the dioxotetraaza macrocycles, the smallest and less flexible H_2**L1**, with the two amine centers at a shorter distance, exhibits the most acidic amine.

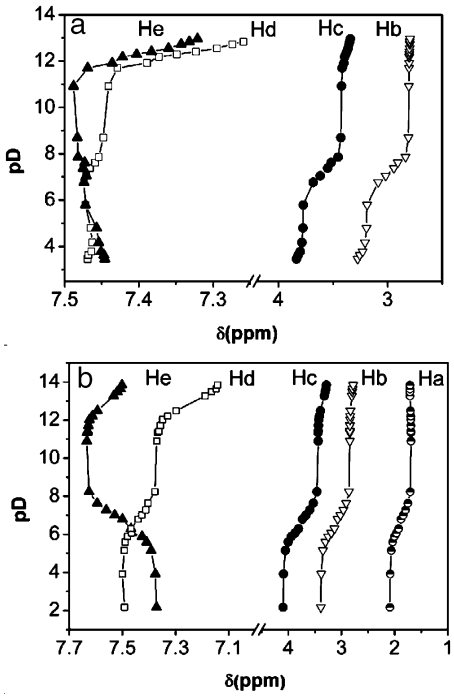

Figure 1. ^{1}H NMR titration curves of H_2**L1** (a) and H_2**L2** (b), for labeling see Scheme 1.

All protonation constants were also determined by ^{1}H NMR titration, Figure 1. The proton spectrum of H_2**L1** consisted of four resonances: two multiplets for four protons were assigned to the aromatic protons, Hd and He, and the macrocyclic methylene protons Hb and Hc appeared as two singlets that correspond to four protons each (see Scheme 1 for proton labeling). For H_2**L2**, the five resonances observed in the proton spectra present two multiplets for the aromatic protons Hd and He that integrate evenly to two protons, a singlet for Hc and a triplet for Hb, with equal intensities (4 H), and a quintuplet that was attributed to Ha, which integrates for two protons. At a pD range of 5.5−6, the spectra show a singlet for the four aromatic protons in both macrocycles, Hd and He.

The ^{1}H NMR titration curves (Figure 1) of the new compounds display the effect of successive protonations of their various basic sites. All the protons involved in the protonation process were used in the refinement of the data in the program HYPNMR,[28] and three protonation constants in D_2O could be determined. The direct conversion of the pK_D values in pK_H was performed using a correlation determined by Delgado et al.[29] for polyaza- and polyoxa-polyaza macrocyclic compounds: $pK_D = 0.11 + 1.10 \times pK_H$. Mindful of the experimental errors on the determination of these values by ^{1}H NMR titration, the obtained protonation constants after conversion to H_2O are comparable to the ones found by potentiometry. In contrast to other cyclic dioxotetraaza macrocycles,[2] the protonation constant of one amide center could be determined because of the aromatic ring introduced near those centers. The first protonation constant was of the same order for the new compounds. By contrast, the presence of two pendent N-acetate functionalities in the H_2**L1** framework (H_4**L6**, see Scheme 1) increases the first protonation constant value to 12.81 as determined by Lacerda et al.[13] This may be associated to hydrogen bond stabilization between one pendent arm and the endocyclic amide and/or to differences in the programs used for calculations.

Albeit these new ligands present comparable protonation profiles in the pH range investigated, H_2**L2** shows larger overall basicity than H_2**L1**; this observation is in accordance with the wider distance between the amine centers in the propylenediamine fragment, which acts to lessen the Coulombic repulsion interactions when both amine centers are protonated.

Stability Constants of Copper Complexes. The stability constants for the formation of copper(II) complexes of H_2**L1** and H_2**L2** were determined in water by potentiometric techniques at 25.0 ± 0.1 °C and at 0.10 ± 0.01 M KNO_3 ionic strength. These values are shown in Table 3 together with those of the same metal complex with other related dioxotetraaza macrocycles.[2]

In agreement with Table 3, both macrocycles, H_2**L1** and H_2**L2**, form only mononuclear complexes with copper(II), namely, $[Cu(HL)]^+$, [CuL], and $[CuL(OH)]^-$. The [CuL] species is formed by the deprotonation of the second amide, for which the protonation constant is unknown; this means the complex with both amides deprotonated. The presence of $[CuL(OH)]^-$ implies the additional loss of one proton from one coordinated water molecule. In the complex $[Cu(HL)]^+$ the more basic amide still remains protonated. In Figure 2 the corresponding species distributions can be seen.

The direct comparison of thermodynamic stability constants of complexes of different ligands can lead to incorrect interpretations as the differences in their basicities are not taken into account. Therefore, to compare values with the related compounds H_2**L3**−H_2**L5**, Table 3 also includes the values of the resulting constants when considering H_2L as the starting species, which means the ligands with both amide centers protonated.

The determination of pCu (−log $[Cu^{2+}]$) is another way to compare the thermodynamic behavior of different compounds. Indeed, the concentration of the free metal cation represents a direct indication of the ligand−metal affinity with consideration of all involved equilibria.[21] Therefore, the assessment of their stability constants via pM values is employed for specific conditions. The pCu data compiled in Table 3 for the two novel compounds and a dioxotetraaza series of reported complexes revealed that H_2**L2** exhibits the highest value of pCu followed by H_2**L5**, H_2**L4**, H_2**L3,** and, finally, H_2**L1**. Therefore, the introduction of the benzene ring on the backbones of these types of ligands induced a critic modulation in their copper complexation with different outcomes. The 12-membered macrocycles, H_2**L1** and H_2**L3**, which are more rigid and have a smaller cavity size compared to all the others, present the lowest affinity for copper(II), with the less flexible H_2**L1** being the most sterically unsuitable. In contrast, the rigidification of the H_2**L4** structure with one benzene ring to give H_2**L2** resulted in a copper complex that was thermodynamically much more stable and

(29) Delgado, R.; Fraústo da Silva, J. J. R.; Amorim, M. T. S.; Cabral, M. F.; Chaves, S.; Costa, J. *Anal. Chim. Acta* **1991**, *245*, 271.

Table 3. Overall Stability Constants (log $\beta_{Cu_cH_hL_l}$) and pCu Values[a] Determined for the Copper(II) Complexes of $\mathbf{L1}^{2-}$ and $\mathbf{L2}^{2-}$ [b] and also the Values of $\mathbf{L3}^{2-}$–$\mathbf{L5}^{2-}$

equilibrium reaction	$\mathbf{L1}^{2-}$ [c]	$\mathbf{L2}^{2-}$ [c]	$\mathbf{L3}^{2-}$ [d]	$\mathbf{L4}^{2-}$ [d]	$\mathbf{L5}^{2-}$ [d]
$Cu^{2+} + (HL^-) \rightleftarrows [Cu(HL)]^+$	9.17(9)	16.3(1)			
$Cu^{2+} + (HL^-) \rightleftarrows [CuL] + H^+$	2.61(1)	13.86(3)			
$Cu^{2+} + (HL^-) \rightleftarrows [CuL(OH)]^- + H^+$		2.4(6)			
$Cu^{2+} + (H_2L) + H^+ \rightleftarrows [Cu(H_3L)]^{3+}$					11.72
$Cu^{2+} + (H_2L) \rightleftarrows [Cu(H_2L)]^{2+}$			6.56	6.08	8.33
$Cu^{2+} + (H_2L) \rightleftarrows [Cu(HL)]^+ + H^+$	−2.39	4.79	1.31		
$Cu^{2+} + (H_2L) \rightleftarrows [CuL] + 2H^+$	−8.95	2.35	−6.65	−3.47	1.86
$Cu^{2+} + (H_2L) \rightleftarrows [CuL(OH)]^- + 3H^+$		−9.11	−16.00	−14.94	
pCu	5.9	17.1	8.7	10.8	16.1

[a] pCu values calculated with Hyss program, at the following conditions: pH 7.4, 100% excess of free ligand, with $C_L = 2C_M = 1 \times 10^{-5}$ M. [b] T = 25 °C; I = 0.10 M in KNO_3. [c] Values in parentheses are standard deviations in the last significant figures. [d] I = 0.10 M in KCl, ref 2.

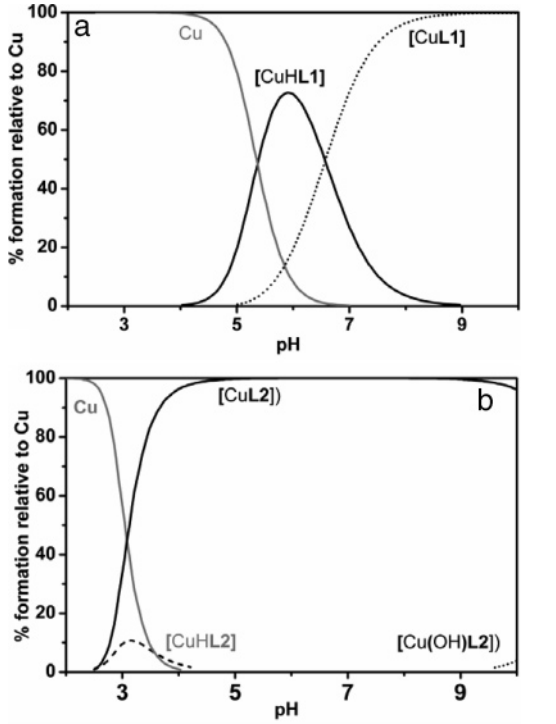

Figure 2. Species–distribution diagram for the copper(II) complexes with H_2**L1** (a) and H_2**L2** (b) in water, $C_L = C_M = 1.0 \times 10^{-5}$ M. Charges are omitted for clarity.

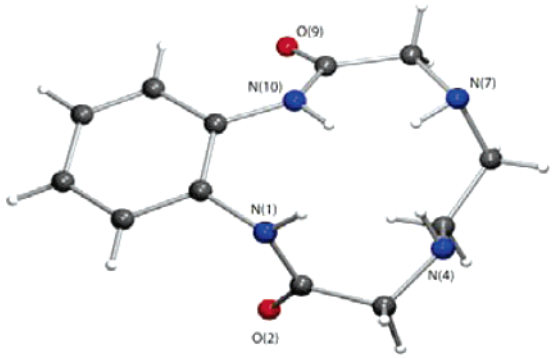

Figure 3. Molecular diagram with the overall structure of the free 12-membered macrocycle H_2**L1**.

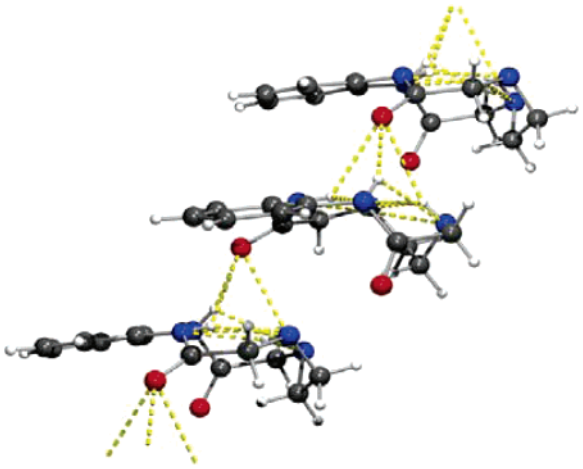

Figure 4. Crystal packing diagram of H_2**L1** showing the formation of the 1D hydrogen-bonding network.

suggests a perfect fit of the copper(II) to the cavity of the macrocycle. Additionally, the high stability constant obtained for H_2**L2** points to a preorganized free ligand in regard to copper(II) complexation, in such a way that low conformational energy is spent in the complexation. The cavity size of H_2**L1** is too small to include the copper(II), and the rearrangement of the donor atoms of this rigid ligand for coordination certainly needs a large amount of energy that is not compensated for in the final structure of the complex. Therefore, the cavity size and geometry of H_2**L2** complement exactly the targeted metal ion and lead to the exceptional thermodynamic stability of its copper complex among all of the ligands presented in Table 3.

Structural Studies. Single-Crystal X-ray Structures. The molecular structure of free H_2**L1** presented in Figure 3 shows that the four N–H groups point toward each other with three of them located above the least-squares plane that is defined by the four nitrogen atoms by 0.17(5), 0.38(4), and 0.77(4) Å, respectively. This conformation is stabilized by four N–H···N hydrogen bonding interactions with H···N distances ranging from 2.11 to 2.53 Å. In the crystal structure the molecules of H_2**L1** are self-assembled into a one-dimensional (1D) chain through the formation of three independent N–H···O hydrogen bonds between one carbonyl group and three N–H binding sites of neighboring molecules with two H···O distances of 2.57 Å and one of 2.05 Å. The 1D network grows along the [010] crystallographic axis as shown in Figure 4. The detailed molecular dimensions of hydrogen bonds are listed in Table 4 along with those found for the copper complexes.

The molecular structure of the copper complexes [Cu**L1**(H_2O)] and [Cu**L2**] are shown in Figures 5 and 6, respectively, and Table 4 lists the selected bond distances and angles in their

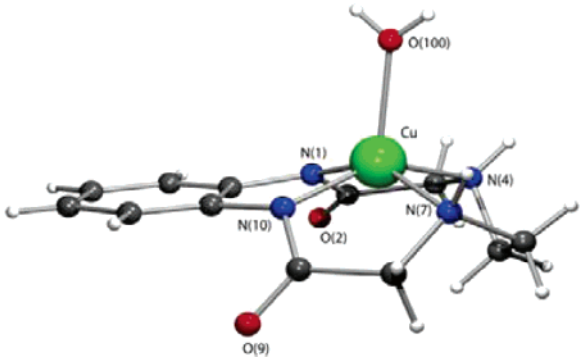

Figure 5. A molecular view of the [Cu**L1**(H_2O)] complex showing the overall structure of the complex and the labeling scheme adopted. For clarity the atomic notation scheme of the carbon atoms is omitted.

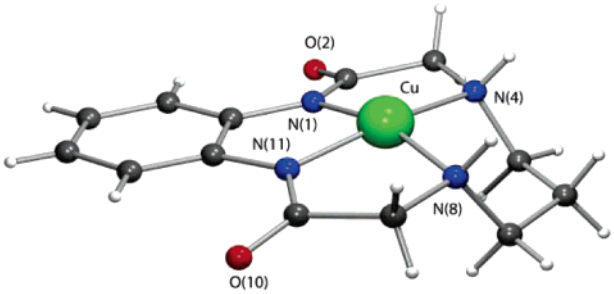

Figure 6. A molecular view of [Cu**L2**] complex. Details as given in Figure 5.

Table 4. Selected Bond Distances (Å) and Angles (°) in the Copper Coordination Sphere of the [Cu**L1**(H_2O)] and [Cu**L2**] Complexes

	[Cu**L1**(H_2O) [$x = 7, y = 10$]	[Cu**L2**] [$x = 8, y = 11$]
Cu−N(1)	1.928(4)	1.9037(17)
Cu−N(4)	2.023(3)	1.9932(18)
Cu−N(x)	2.029(4)	1.9907(17)
Cu−N(y)	1.923(4)	1.9053(17)
Cu−O(100)	2.165(3)	
N(1)−Cu−N(4)	84.81(15)	86.21(7)
N(*y*)−Cu−N(1)	82.92(16)	84.26(7)
N(*y*)−Cu−N(4)	146.11(14)	165.47(7)
N(*y*)−Cu−N(*x*)	84.88(15)	86.46(7)
N(1)−Cu−N(*x*)	148.57(15)	163.61(8)
N(4)−Cu−N(*x*)	89.47(14)	100.03(7)
N(1)−Cu−O(100)	108.12(16	
N(4)−Cu−O(100)	100.84(15)	
N(*x*)−Cu−O(100)	103.31(15)	
N(10)−Cu−O(100)	112.98(15)	

coordination spheres. The copper in the complex [Cu**L1**(H_2O)] shows a distorted square−pyramidal geometry with the copper center located 0.552(2) Å above the N_4 macrocyclic plane and toward the apical coordination water that leads to a Cu−O distance of 2.165(3) Å. Consequently, the distance of the bound water molecule from the N_4 coordination plane is 2.706(4) Å. The copper in the complex [Cu**L2**] exhibits a square−planar coordination with the metal center located only 0.180(1) Å away from the N_4 equatorial coordination plane. In spite of the inherent structural differences between the two coordination geometries, this comparison clearly suggests that the larger 13-membered macrocycle has enough room to accommodate the copper(II) metal center, and the 12-membered ring has a smaller cavity size that has the metal center located out of the macrocyclic N_4 coordination plane. A search for X-ray structures of H_2**L1** and H_2**L2** framework

Table 5. Dimensions of the Hydrogen Bonds

	H···A/Å	D···A/Å	D−H···A /°
free ligand H_2**L1** **1**			
N(1)−H(1)···O(9)	2.06(5)	2.864(5)	157(6)
N(4)−H(4)···N(1)	2.60(3)	3.006(5)	112(3)
N(4)−H(4)···N(7)	2.53(2)	2.951(5)	112.5(19)
N(4)−H(4)···O(9) [−1/2 + *x*, 3/2 − *y*, *z*]	2.06(5)	2.864(5)	157(6)
N(4)−H(4)···O(9) [−1/2 + *x*, 3/2 − *y*, *z*]	2.57(3)	3.339(4)	154(3)
N(7)−H(7)···N(4)	2.50(4)	2.951(5)	114(4)
N(7)−H(7)···N(10)	2.11(5)	2.782(5)	135(4)
N(10)−H(10)···N(1)	2.39(5)	2.777(5)	108(4)
N(10)−H(10)···N(7)	2.31(5)	2.782(5)	115(4)
N(10)−H(10)···O(9)	2.57(4)	3.194(5)	130(4)
[Cu**L1**(H_2O)] **2**			
N(4)−H(4)···O(2) [1 − *x*, 1/2 + *y*, 2 − *z*]	2.31	2.988(5)	131
N(7)−H(7)···O(9)	2.04	2.935(5)	166
O(100)−H(101)···O(2) [2 − *x*, 1/2 + *y*, 2 − *z*]	2.09(5)	2.828(5)	151(5)
O(100)−H(102)···O(200) [*x*, 1 + *y*, *z*]	1.89(3)	2.667(6)	158(6)
O(200)−H(202)···O(2)	2.06(4)	2.869(5)	171(5)
[Cu**L2**] **3**			
N(4)−H(4)···O(10) [3/2 − *x*, 1/2 + *y*, 1/2 − *z*]	2.03	2.933(2)	175
N(8)−H(8)···O(100) [3/2 − *x*, 1/2 + *y*,1/2 − *z*]	2.05	2.929(3	163
O(100)−H(101)···O(2) [3/2 − *x*, −1/2 + *y*, −1/2 − *z*]	1.931(13)	2.729(2)	171(3)
O(100)−H(102)···O(10)	2.015(18)	2.815(2)	173(2)

derivatives on the Cambridge crystallographic database (CSD)[30] provided only three structures of H_2**L1** derivatives: the copper(II) complexes of H_4**L6** (Refcode CADGEU)[31] and H_2**L7** (Refcode KALPUJ).[13] The third structure corresponds to H_3**L6**$^-$ (Refcode CADGAQ).[31] Both copper complexes have octahedral coordination environments with only the two sp^3 nitrogen donors and the oxygen atom from a carbonyl group bonded to the metal center. By contrast, in the two complexes described here the four nitrogen atoms coordinate to the copper center with similar Cu−N distances. Furthermore, the two Cu−N distances of sp^3 nitrogen donors are ca. 0.1 Å longer than those involving the two amide nitrogen atoms. Finally, the benzene ring is almost coplanar with the N_4 coordination plane and forms a dihedral angle of only 2.8° in both complexes. In the free ligand H_2**L1**, this angle increases to 16.1°.

The dimensions of all hydrogen bonding interactions found for [Cu**L1**(H_2O)] and [Cu**L2**] are listed in Table 5. The crystal structures of [Cu**L1**(H_2O)] and [Cu**L2**] are built up from asymmetric units composed of the respective complexes and one water solvent molecule. As found for the free ligand H_2**L1**, the copper(II) complex molecules [Cu**L1**(H_2O)] and [Cu**L2**] are self-assembled via N−H···O hydrogen bonds leading to the formation of 1D chains, which are further connected by O−H···O and N−H···O with water solvent molecules that lead to the formation of two- and three-dimensional (2D and 3D, respectively) networks of hydrogen

(30) (a) Allen, F. H. *Acta. Crystallogr*. **2002**, *B58*, 380. (b) Bruno, I. J.; Cole J. C.; Edginton, P. R.; Kessler, M.; Macrae, C. F.; McCabe, P.; Pearson, J.; Taylor, R. *Acta. Crystallogr*. **2002**, *B58*, 389.
(31) Inoue, M. B.; Machi, L.; Munoz, I. C.; Rojas-Rivas, S.; Inoue, M.; Fernando, Q. *Inorg. Chim. Acta* **2001**, *324*, 73.

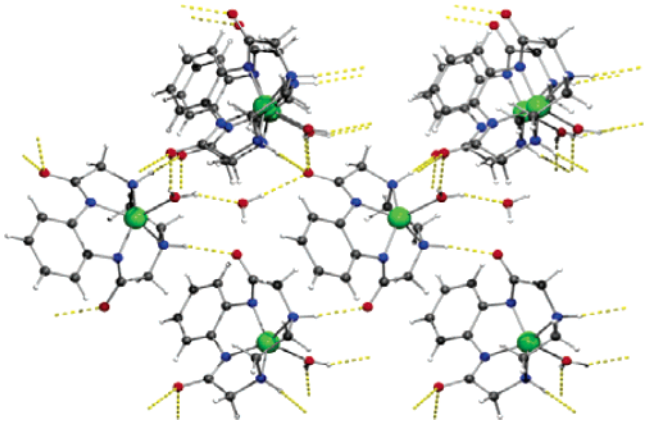

Figure 7. Crystal packing diagram of [Cu**L1**(H_2O)].

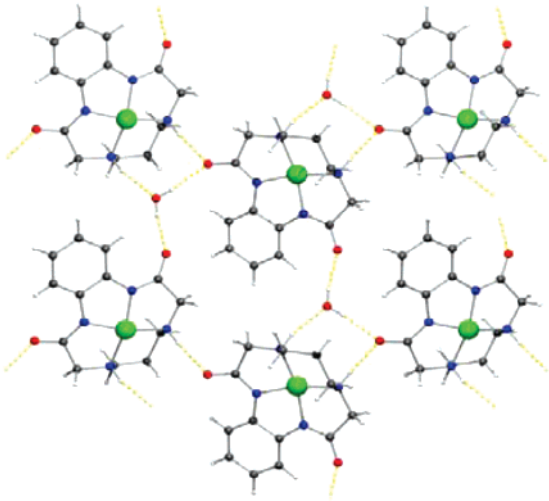

Figure 8. Crystal packing diagram of [Cu**L2**].

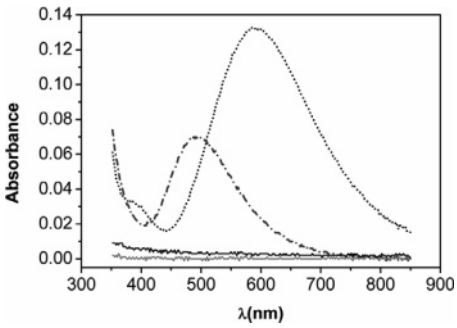

Figure 9. Electronic spectra of aqueous solutions of H_2**L1** (gray) and H_2**L2** (black), and the [Cu**L1**(H_2O)] (dots) and [Cu**L2**] (dashes and dots) complexes at pH 7.8 and 6.5, respectively.

bonds for [Cu**L1**(H_2O)] and [Cu**L2**], respectively. In addition, in the complex [Cu**L2**], O−H···O hydrogen bonds were also found between the coordinated and solvent water molecules (see Table 5). Perspective views of crystal packing diagrams of [Cu**L1**(H_2O)] and [Cu**L2**] are shown in Figures 7 and 8, respectively.

Spectroscopic Studies in Solution with Copper Complexes. The electronic spectra of copper complexes of H_2**L1** and of H_2**L2** in aqueous solution at different pH values present dissimilar features (Figure 9 and Table 6). The [Cu**L1**] complex shows an obvious spectral modification from acidic to alkaline solutions, which differs from the

Table 6. Color and Spectroscopic Data for the [Cu**L1**] and [Cu**L2**] Complexes

complex	color	pH	λ / nm (ϵ_{molar} / [$dm^3 \cdot mol^{-1} \cdot cm^{-1}$])[a]
Cu**L1**	blue	4.4	408 (140), 608 (450), 756 (sh., 200)
		5.2	406 (280), 596 (1170), 732 (sh., 510)
		7.8	406 (270), 584 (1330), 736 (sh., 500)
		10.8	406 (260), 588 (1280), 736 (sh., 480)
Cu**L2**	pink	2.3	496 (260), 592 (sh., 100)
		6.5	496 (700), 592 (sh., 260)
		10.0	496 (640), 592 (sh., 240)

[a] sh. = shoulder.

[Cu**L2**] complex where no shift of the absorption maximum of the d−d transition band could be identified. The [Cu**L1**] ligand shows one main species, [Cu**L**], in the pH range studied (see Figure 2). Similarly to other copper complexes of dioxotetraaza macrocycles such as Cu_2**L4** or H_2**L5**, [Cu**L2**] displays a single d−d transition band in the 500−650 nm region, with the maximum achieved at 592 nm.[2] The conformational strain in the H_2**L1** backbone leads to high values of the absorption coefficient and blue shifts of the d−d band of its copper(II) complex as the pH rises. This is what was previously observed for [Cu**L3**] or with other 12-membered rings of this class of compounds.[2,32] In particular, the hypsochromic shift observed for the [Cu**L1**] complex is ascribed to an increment in the ligand field strength that suggests the coordination of an additional donor atom to the metal center, which is related to the yield of two main species: $[CuH\mathbf{L1}]^+$ and [Cu**L1**] as the pH increases (Figure 2). These results indicate that the [Cu**L1**] complex displays a weaker metal−ligand interaction and a more distorted geometry as compared to the [Cu**L2**] complex, which is due to the H_2**L1** rigidity and a cavity size that is less suitable to encapsulate the copper(II) in the N_4 plane. Nevertheless, the information given by the electronic spectra is not sufficient to assign the detailed coordination geometry of copper(II) complexes.

The EPR spectra of the Cu**L1** and the Cu**L2** complexes were performed in DMSO/H_2O 1:1 v/v solutions at 96 K, which showed the presence of only one species, see Figure 10. The spectra exhibit four well-resolved lines, as is expected for the unpaired electron density of the copper(II) nucleus. Superhyperfine splitting due to coupling with the donor atoms of the macrocycle has not been observed. The hyperfine coupling constants (A) and g values obtained by simulation[33] of the EPR spectra are gathered in Table 7. The anisotropic spectral morphology ($g_x \neq g_y \neq g_z$) found is typical of mononuclear copper(II) complexes with the metal in a rhombically distorted ligand field. Both copper complexes have g_z/A_z values of about 100 cm^{-1} that fall in the usual range for square−planar complexes (g_z/A_z = 105−135 cm^{-1}). These results are in agreement to those determined for the copper complexes of other dioxotetraaza macrocycles which were proposed to have the square−planar

(32) Hay, R. W.; Bembi, R.; Sommerville, W. *Inorg. Chim. Acta* **1982**, *59*, 147.
(33) Neese, F. Diploma Thesis, University of Konstanz, Germany, 1993.

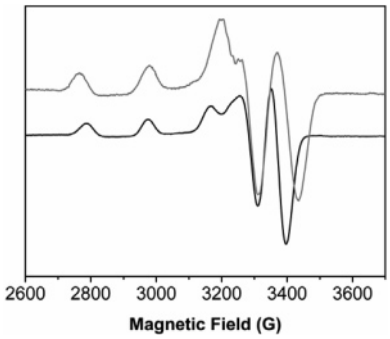

Figure 10. X-band EPR spectra of the [Cu**L1**(H_2O)] (bottom) and [Cu**L2**] (top) complexes in DMSO/H_2O 1:1 v/v and in 1.0 M $NaClO_4$ at pH 10. The spectra were recorded at 96 K with a microwave power of 2.0 mW and a modulation amplitude of 1 mT. The frequencies were 9.414 and 9.404 GHz, respectively.

Table 7. EPR Data for the [Cu**L1**(H_2O)] and [Cu**L2**] Complexes at pH 10

	EPR parameters ($A/10^4$ cm^{-1})					
copper(II) complex	g_x	g_y	g_z	A_x	A_y	A_z
[Cu**L1**(H_2O)]	2.038	2.052	2.193	0.32	14.97	193.12
[Cu**L2**]	2.018	2.058	2.166	5.28	18.64	209.01

configuration.[2,34] Moreover, the comparison of copper complexes of small peptides, such as Gly−Gly−Gly−Gly, by a Peisach−Blumberg[35] diagram, shows that both the Cu**L1** and the Cu**L2** complexes fall inside of the area of the square−planar structures. However, the complex of the 12-membered ring holds a smaller A_z parameter, larger g_z parameter, and exhibits an electronic spectrum with a red shift in regard to the Cu**L2** complex. On the basis of these findings, a square−pyramidal structure at high pH is predicted for Cu**L1** where the planar ligand field becomes weaker or an axial ligand field becomes stronger. These results indicate that the structures of the copper complexes in solution and in the crystal state are identical.

Radiochemistry. The optimal conditions used to prepare the ^{67}Cu−complexes of the two novel compounds are summarized in Table 8. The specific activities were not optimized to achieve their maximum value. Although ^{67}Cu**L1** could not be prepared with high radiochemical yield, ^{67}Cu**L2** was effectively labeled in different conditions. This is consistent with the thermodynamic stability constants and pCu values determined for both ligands. The Cu**L1** complex presented the lowest pCu value, and its labeling with ^{67}Cu provided a yield of 13%, even at 95 °C, with an incubation time of 60 min. The high pCu value for Cu**L2** correlates with its effective labeling with ^{67}Cu (yield > 98%), which was achieved under the following conditions: pH 8 and RT after 15 min, pH 5.5 and 39 °C after 15 min, and pH 5.5 and 95 °C after 5 min. In contrast to H_2**L2**, its parent compound H_2**L4** has a poor labeling yield with about 4% of ^{67}Cu at pH 5.5 and 37 °C after 20 h of incubation time.[5] This can be associated to the relatively minor pCu value for the [Cu**L4**] complex with regard to the value of [Cu**L2**].

The suitability of H_2**L2** for its coupling to a biomolecule such as an antibody seems to be feasible because the labeling with ^{67}Cu was performed under mild conditions. The high labeling efficiency for H_2**L2** allowed us to proceed with its characterization and in vitro stability studies.

Table 8. Labeling Conditions for H_2**L1** and H_2**L2** with $^{67}CuCl_2$

ligand	specific activity (mCi/mg)	pH[a]	T (°C)	incubation time (min)	radiochemical purity (%)[b]
H_2**L1**	2.5[c]	8.0	25	1440	30.6
	1.0[c]	8.0	95	60	13.0
	2.5[c]	6.4	25	1440	0
	2.5[c]	6.4	95	60	5.0
	2.5[c]	5.5	25	1440	0
	2.5[c]	5.5	95	60	4.3
H_2**L2**	2.5[c]	8.0	25	15	98.0
	2.5[c]	6.4	25	30	91.4
	2.5[c]	5.5	25	90	91.2
	2.5−3.2[c]	5.5	39	15	100
	2.5−5.0[d]	5.5	95	5	100

[a] 0.1 M ammonium acetate buffer. [b] By analytical HPLC, elution system: flow: 0.75 mL/ min; A, 10% ammonium acetate in H_2O; B, MeOH; gradient: 0−5 min 50% B, 5−10 min 50−100% B, 10−15 min 100% B, 15−20 min 100−50% B. [c] Chelator concentration used: 5×10^{-3} M. [d] Chelator concentrations used: 5×10^{-3} M and 1×10^{-3} M.

The determination of partition coefficient values at physiological pH for the radioligand H_2**L2** was performed using the shake−flask method between octanol and PBS (pH 7.4). The log D value of -0.19 ± 0.03 infers a slight hydrophilic character to the [^{67}Cu**L2**] complex.

A first perception of the radioactive complex stability can be acquired by several in vitro stability studies in physiological media, by competition with other chelators or metals, and, most importantly, by assessment of its serum stability. In this sense, the radiocopper complexes were incubated for 5 days in saline solution, PBS (pH 7.4), 0.1 M tris buffer (pH 7.4), several solutions of 0.1 M ammonium acetate at different pH (5.5, 6.4 and 8), and fresh human serum. Also, some competition experiments with a 100-fold excess of DTPA and copper(II) were performed. In all of the stability experiments with ^{67}Cu labeled to H_2**L2**, the aliquots were analyzed by analytical HPLC to give the intact radiocomplex, even after 5 days. In parallel, the bound serum protein was determined, and about 6% of the radioligand was found in the proteic fraction in a time-independent manner. [^{67}Cu-DTPA] could not be detected on the analytical HPLC by the addition of an excess of DTPA to the proteic fraction at the 2 h time point. These observations strongly indicate that no transchelation has taken place; therefore, we can only speculate that another type of binding between the radiocomplex and the serum proteins has occurred.

Conclusions

The two-step synthesis of the new 12- and 13-membered benzodioxotetraaza macrocycles was achieved in high yield. The coordination of these ligands with copper(II) afforded complexes where the metal center adopts a distorted square−pyramidal geometry in [Cu**L1**(H_2O)] and a distorted square−planar based structure in [Cu**L2**]. The copper(II) complex with H_2**L1**, the most rigid ligand because of its small cavity size and the presence of the benzene ring in its framework, showed a very low stability constant. By contrast, H_2**L2** has the right cavity size for the fitting of the copper(II), and it

(34) Zhu, S.; Kou, F.; Lin, H.; Lin, C.; Chen, Y. *Inorg. Chem.* **1996**, *35*, 5851.
(35) Peisach, J.; Blumberg, W. E. *Arch. Biochem. Biophys.* **1974**, *165*, 691.

has a preorganized topology for the encapsulation of this metal center, which leads to the most thermodynamically stable complex among the dioxotetraaza macrocycles.

The H_2**L2** was labeled successfully with ^{67}Cu (yield > 98%) in correlation with its high pCu value. The radioligand H_2**L2** was stable in saline solution, PBS (pH 7.4), tris buffer (pH 7.4), 0.1 M ammonium acetate (pH 5.5 or 6.5 or 8.0), with a 100−fold excess of DTPA, and with a 50−fold excess of copper(II). The intact radioligand was also found in serum stability studies, albeit its 6% of bound serum protein.

On the basis of these global promising findings regarding the [^{67}Cu**L2**] complex, in vivo stability and the pharmacokinetic profile are necessary to confirm its future applicability in nuclear medicine.

Acknowledgment. The authors acknowledge the financial support from Fundação para a Ciência e a Tecnologia (FCT) and POCTI, with co-participation of the European community fund FEDER (Project N*o*. POCTI/2000/CBO/35859) and from Swiss National Science Foundation project 3100A0-100390, BBW No. C00.0091 and BBT project 4668.1 EUS. P. A. also acknowledges the Ph.D. fellowship of the FCT, SFRH/BD/3136/2000. The authors also thank EPSRC and the University of Reading for funds for the X-Calibur system. The support provided by Novartis Pharma with respect to ESI−MS analysis is gratefully acknowledged. Silvia Carvalho is acknowledged for the EPR spectra acquisition. The authors are grateful for the $^{67}CuCl_2$ gift from PSI.

Supporting Information Available: Crystallographic data in CIF format. This material is available free of charge via the Internet at http://pubs.acs.org.

IC062172O